



OPEN ACCESS

EDITED BY

Alessandro Bergamasco,
National Research Council (CNR), Italy

REVIEWED BY

Veljko Srzić,
University of Split, Croatia
Mohammed Benaafi,
King Fahd University of Petroleum and
Minerals, Saudi Arabia

*CORRESPONDENCE

Chaoyue Wang
✉ wangchaoyue08@163.com

RECEIVED 09 February 2024

ACCEPTED 29 April 2024

PUBLISHED 16 May 2024

CITATION

Li H, Liu Y, Wang C, Yu K, Zhou Y, Fu X, Bai X
and Li X (2024) Hydrogeochemical
characteristics of shallow groundwater
and salinization evaluation in the coastal
aquifers of Cangzhou, China.
Front. Mar. Sci. 11:1384289.
doi: 10.3389/fmars.2024.1384289

COPYRIGHT

© 2024 Li, Liu, Wang, Yu, Zhou, Fu, Bai and Li.
This is an open-access article distributed under
the terms of the [Creative Commons Attribution
License \(CC BY\)](https://creativecommons.org/licenses/by/4.0/). The use, distribution or
reproduction in other forums is permitted,
provided the original author(s) and the
copyright owner(s) are credited and that the
original publication in this journal is cited, in
accordance with accepted academic
practice. No use, distribution or reproduction
is permitted which does not comply with
these terms.

Hydrogeochemical characteristics of shallow groundwater and salinization evaluation in the coastal aquifers of Cangzhou, China

Hui Li^{1,2,3}, Yang Liu⁴, Chaoyue Wang^{1,5*}, Kaining Yu^{1,5},
Yahong Zhou^{1,5}, Xiaogang Fu^{1,5}, Xiaoli Bai⁶ and Xin Li⁷

¹Hebei Center for Ecological and Environmental Geology Research, Hebei GEO University, Shijiazhuang, China, ²The Sixth Geological Brigade of Geological Mineral Exploration and Development Bureau of Hebei Province, Shijiazhuang, China, ³Aerial Measurement Technology Application Research Center Under the Geological Mineral Exploration and Development Bureau of Hebei Province, Shijiazhuang, China, ⁴Hebei Key Laboratory of Geological Resources and Environment Monitoring and Protection, Hebei Geo-Environment Monitoring Institute, Shijiazhuang, China, ⁵Hebei Province Collaborative Innovation Center for Sustainable Utilization of Water Resources and Optimization of Industrial Structure, Hebei GEO University, Shijiazhuang, China, ⁶Hebei Vocational and Technical College of Resources and Environment, Shijiazhuang, China, ⁷Land Resources Exploration Center, Geological Mineral Exploration and Development Bureau of Hebei Province, Shijiazhuang, China

To investigate the hydrogeochemical characteristics of shallow groundwater and evaluate groundwater salinization state in Cangzhou, China, two sampling campaigns have been conducted. In summer, 33 groundwater samples, 3 seawater samples and 5 river water samples were collected. In winter, 22 groundwater samples were collected. The hydrochemical type was determined by the Piper diagram. Evolution mechanisms of groundwater were analyzed by the Gibbs diagram. The trend of de-salinization or salinization of groundwater was determined by the hydrochemical facies evolution diagram. The groundwater salinization grade was evaluated by both the seawater intrusion groundwater quality index (GQI_{SWI}) and the attribute recognition model based on entropy weight (ARMEW). The Piper diagram shows that Na^+ is the dominant cation and Cl^- is the dominant anion in shallow groundwater, and the groundwater in this area is mainly of Cl-Na type followed by Cl-Ca-Mg type. The evaporation-crystallization process has significant influence on the evolution of saline groundwater. In summer, most brackish groundwater exhibit compositions of the freshening stage with direct cation exchange, and most saline groundwater is mainly at the seawater intrusion stage with reverse cation exchange. In winter, compared to the summer season, more groundwater samples in the middle of study area exhibit intrusion trend, and without obvious Na- HCO_3 facies. In summer, values of GQI_{SWI} range from 20.47 to 75.38 with an average of 59.31. The GQI_{SWI} gradually increases from east to west, denoting the degree of groundwater salinization is alleviated from coast to inland. In winter, values of GQI_{SWI} range from 54.47 to 79.09 with an average of 66.00, slightly higher than that in summer. The proportion of no salinization (Grade I), minor salinization (Grade II) and serious salinization (Grade III) of groundwater samples in Cangzhou identified by ARMEW is 3.0%, 21.2% and 75.8% in summer, respectively. In winter, the proportion is 9.1% for Grade II and 90.9% for Grade III. The GQI_{SWI} index shows the largest area of Grade II, and

ARMEW presents the largest area of Grade III in both seasons. Compared with GQI_{SWI} index, ARMEW model gives more conservative evaluation results of groundwater salinization. The results provide useful information on the groundwater salinization status for the local area, and help for the management of groundwater resources in Cangzhou.

KEYWORDS

groundwater salinization, hydrochemical characteristics, seawater intrusion, groundwater quality index, attribute recognition model based on entropy weight, Cangzhou

1 Introduction

Groundwater is one of the crucial resources for coastal areas which accommodate 40% of the world's population (Essink, 2001). Nevertheless, growing population and city expansion have exerted enormous stress on groundwater quantity (Kumar et al., 2023). The excessive exploitation of groundwater has caused many problems including seawater intrusion, soil salinization, worsened groundwater quality and ecological deterioration (Stamatis and Voudouris, 2003; Bless et al., 2018; Li et al., 2022; Xiong et al., 2022).

Groundwater salinization is becoming one of the major environmental issues in more and more coastal areas around the world, and about 32% of the coastal metropolitan cities have been threatened. It is reported that over 501 cities around the world facing groundwater salinization issues (Cao et al., 2021). Many countries have paid much attention to the research of groundwater salinization, including USA (Jasechko et al., 2020; Lotfata and Ambinakudige, 2020), UK (Moulds et al., 2023), Korea (Kim et al., 2021), Australia (Banks et al., 2021), India (Dhakate et al., 2020), Spain (Martínez-Pérez et al., 2022), Italy (Ghiglieri et al., 2012), Saudi Arabia (Benaafi et al., 2022, 2023) and Tunisia (Moussaoui et al., 2023).

To evaluate regional groundwater salinization status, chemical indexes such as Cl^- or total dissolved solids (TDS) are commonly used. Compared to the single-index method, the multi-index evaluation method has obvious advantages, which can reflect the groundwater salinization degree more comprehensively and stably. The multi-index evaluation method includes the GALDIT method (ChaChadi and Lobo-Ferreira, 2001), the "water quality index" (WQI) method (Boyacioglu, 2007), the groundwater quality index for seawater intrusion (GQI_{SWI} , Tomaszekiewicz et al., 2014), fuzzy mathematics (Zhao, 1998; Icaga, 2007), analytic hierarchy process (Saaty, 1980), and entropy weight method (Zou et al., 2006). Wherein, the GQI_{SWI} incorporates the seawater proportion and information from the Piper graph to convert groundwater chemical types into numerical values (0~100). Therefore, it can directly evaluate the degree of groundwater salinization by values of GQI_{SWI} , which is more comprehensive than the single-index

method. Besides, for the entropy weight method, it has obvious advantages in calculating index objective weights. However, entropy weights are easily influenced by sample size and value. Also, it depends excessively upon objective data when determining weights, and ignores the relation between objectives and indicators. This sometimes leads to confusing and unexplained assessments (Wang et al., 2022).

To address these limitations, here, the entropy weight method was coupled with the attribute recognition model which fully considers the sample information. In this method, the index weights are determined by the judgment matrix related to representative values for evaluation indices under objective conditions. It combines the objective weighting characteristics of entropy weight method with the ordered segmentation of attribute recognition model. By this means, the subjectivity of the weight of each factor is eliminated, and the evaluation results are in accord with the fact. Therefore, to assess groundwater salinization status, this study applied both the GQI_{SWI} index and the attribute recognition model based on entropy weight (ARMEW).

In China, groundwater salinization research has been reported for coastal aquifers near the Jiaozhou Bay (Gang et al., 2019), the Yellow River delta (Liu et al., 2014), the Laizhou Bay (Xue et al., 1993; Han et al., 2011; Wang et al., 2020), the Qianhuangdao area (Zhang et al., 2013), and the southern China (Xiong et al., 2022). However, there were few studies investigating the hydrogeochemical characteristics and groundwater salinization in the coastal region of Cangzhou on the west of Bohai Bay. Groundwater salinization status was seldom investigated for this important area that 7.54 million people inhabit. In addition, although different evaluation methods have been put forward in previous work, few studies compared the salinization results between different evaluation methods. To fill these gaps, the present study tries to conduct a detailed and a systematic evaluation on the groundwater salinization status and related hydrogeochemical characteristics through multidisciplinary methods. The main goals of this work include: (1) identify shallow groundwater hydrogeochemical characteristics and its evolution mechanisms; (2) assess and compare the degree of groundwater salinization through both methods of GQI_{SWI} index

and the ARMEW. The results provide useful information on the groundwater salinization status for the local area, and help for the management of groundwater resources.

2 Materials and methods

2.1 Study area

Cangzhou City is located in the east of Hebei Province, China, with an area of 14,304 km² (Figure 1). The climate in this area is controlled by the warm temperate continental monsoon, with four distinct seasons. The annual average temperature is 12.5°C. The annual average precipitation is 581 mm and the annual average evaporation is 1,574 mm. The precipitation in July to September accounts for 66% of the annual precipitation. The terrain in this region is flat with the general elevation lower than 16 m, and it inclines slightly from southwest to northeast. The South Canal, part of the Beijing-Hangzhou Canal, flows through this area. Other main rivers include the Ziya River, the Jiedjian River, the Nanpai Canal, the Dalangdian Canal, and the Xuanhui River.

The hydrogeological unit of shallow aquifer in this region is classified into three types (Figure 1, Xu, 2009) the alluvial plain (①), the sedimentary plain formed by the land-sea interaction (②) and the coastal plain (③). From inland to sea, the sediments of aquifers change from fine sand to silt. From top to bottom, the quaternary aquifers in Cangzhou area is categorized into 4 groups (Figure 2). In this study, we focus on the aquifer I, which consists of Holocene loose sediments with a bottom depth of 20~30 m (Chen et al., 2015).

The aquifer receives recharge mainly from atmospheric precipitation. Groundwater is discharged mainly through evaporation and extraction. Under the natural state, the groundwater flow direction is in accordance with the terrain

slope, that is, from southwest to northeast. The flat terrain with the small hydraulic gradient result in a slow movement of groundwater. Compared with the western regions, groundwater in the coastal areas is almost stagnant. It is reported that from 1990 to 2015, the average groundwater depth in this region first increased, then decreased, from the initial 3.26 to 4.06 m (Yan et al., 2021).

Brackish water is widely distributed within this area. The thickness of the brackish water shrinks gradually from coast toward inland (Figure 2), forming a wedge between the shallow freshwater and the deep freshwater. The formation of the brackish water in Cangzhou result from combined effects of various factors such as paleoclimate conditions, paleogeographic and geological environment and transgressions in the Quaternary period. For example, the dry climate in the late Pleistocene serve as the decisive factor for the formation of brackish water in aquifer group II. In addition, it is reported that Cangzhou has experienced seven transgressions in the quaternary period (Xu et al., 2009). Due to the influence of transgressions and tides, a large amount of salt brought by seawater stayed in the loose sedimentary layer. On the other hand, the residual seawater is preserved in the aquifer during the regression, resulting in an increase in the total dissolved solids (TDS), which directly affected the chemical composition of local groundwater.

2.2 Sample collection and analysis

Two sampling campaigns were conducted. In summer (May~June 2022, wet season), we collected 33 groundwater samples, 3 seawater samples and 5 river water samples. In winter (December~January, dry season), 22 groundwater samples were collected (Figure 1). Locations and ground elevations of the sampling sites were recorded using the RTK (South Yinhe1) device. All groundwater samples were taken from the loose

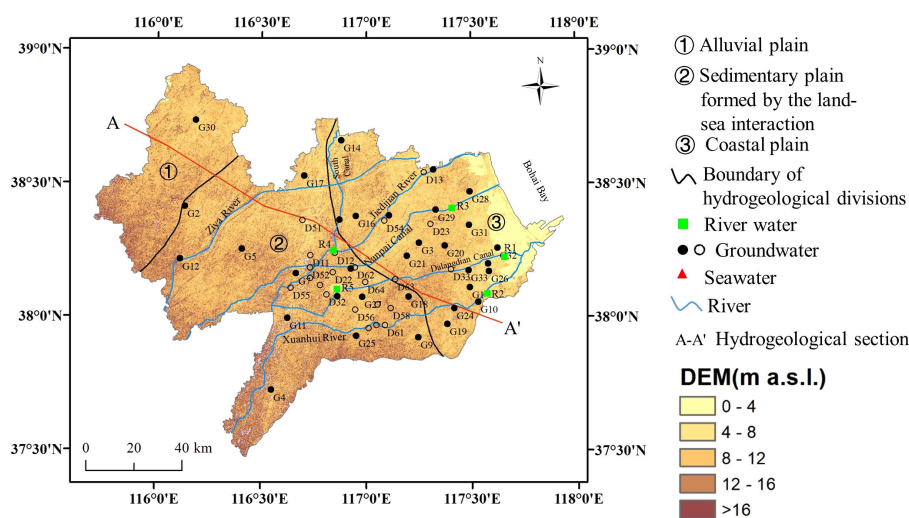


FIGURE 1 Map of research location with sampling points in Cangzhou, China. Solid black circles denote groundwater samples collected in summer and hollow circles denote groundwater samples collected in winter.

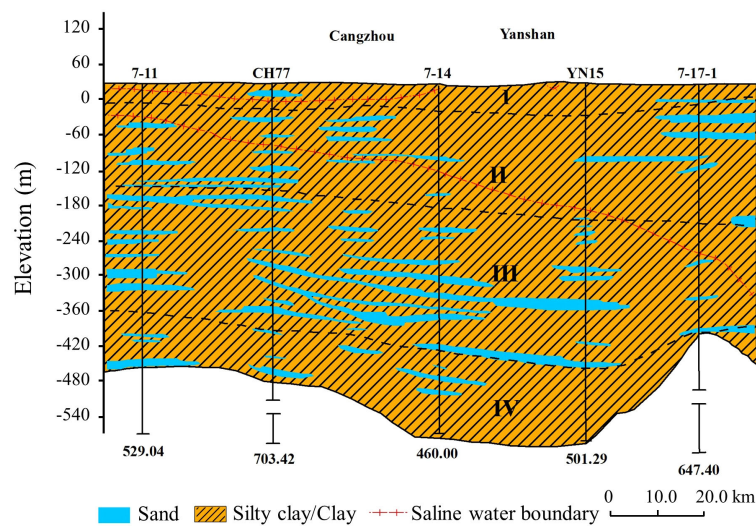


FIGURE 2
Hydrogeological profile of A-A', Cangzhou area, Hebei Province, China.

Quaternary porous aquifer I. The depth of wells changes from 4 m to 30 m, and the sampling depths range from one to ten meters. Before sampling, wells were pumped for 5-10 min to avoid stagnant water in the pipeline. Surface water were collected 0.2 m below the water surface. All samples were filtered through a 0.45 μm membrane, and stored in a polyethylene plastic bottle (500 mL). The sampling bottles were sealed, refrigerated at 4 $^{\circ}\text{C}$ and transported to the Groundwater Mineral Water and Environmental Monitoring Center, Ministry of Land and Resources for water quality analysis. Values of pH were determined by the glass electrode method. Major cations of K^+ , Ca^{2+} , Na^+ , Mg^{2+} were examined by ICP-AES (iCAP 6300). Major anions of HCO_3^- and CO_3^{2-} were examined by titration, and SO_4^{2-} and NO_3^- were determined by the ion chromatographic method. The Cl^- was examined by the silver nitrate volumetric method. All indexes were measured strictly according to the standard for groundwater quality of the People's Republic of China (GB/T 14848-2017). The data reliability was checked by the charge balance error, with all errors within $\pm 7\%$ (Supplementary Table S1).

2.3 Seawater intrusion groundwater quality index

The index of GQI_{SWI} (Equations 1–5) proposed by Tomaszewicz et al. (2014) was used for seawater intrusion.

$$f_{\text{sea}} = \frac{m_{\text{Cl}}(\text{sample}) - m_{\text{Cl}}(\text{freshwater})}{m_{\text{Cl}}(\text{seawater}) - m_{\text{Cl}}(\text{freshwater})} \quad (1)$$

$$\text{GQI}_{\text{Piper}(\text{mix})} = \left[\frac{(\text{Ca}^{2+} + \text{Mg}^{2+})}{\text{Total cations}} + \frac{(\text{HCO}_3^-)}{\text{Total anions}} \right] \times 50 \text{ (in meq/l)} \quad (2)$$

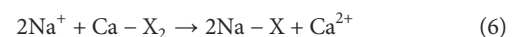
$$\text{GQI}_{\text{Piper}(\text{dom})} = \left[\frac{(\text{Na}^+ + \text{K}^+)}{\text{Total cations}} + \frac{(\text{HCO}_3^-)}{\text{Total anions}} \right] \times 50 \text{ (in meq/l)} \quad (3)$$

$$\text{GQI}_{f_{\text{sea}}} = (1 - f_{\text{sea}}) \times 100 \quad (4)$$

$$\text{GQI}_{\text{SWI}} = \frac{\text{GQI}_{\text{Piper}(\text{mix})} + \text{GQI}_{f_{\text{sea}}}}{2} \quad (5)$$

2.4 Hydrochemical facies evolution diagram

The hydrochemical facies evolution diagram (HFE-D) acts as a useful tool to identify whether the aquifer is in the stage of sea water intrusion or freshening (Giménez-Forcada, 2010). It highlights 4 typical facies (Na-HCO_3 , Na-Cl , Ca-HCO_3 and Ca-Cl) from 16 facies. During the intrusion process, the increasing groundwater salinity (Equation 6) induces inverse exchange reactions, forming the characteristic Ca-Cl facies. Further, the groundwater evolves into seawater (Na-Cl). In the freshening stage, freshwater recharge causes direct exchange reactions, forming the Na-HCO_3 facies. Then the water composition gradually gets similar to that of recharge water and helps the recovery of aquifers.



2.5 Attribute recognition model based on entropy weight

The steps of establishing the ARMEW (Cheng, 1997; Zhang et al., 2010; Li et al., 2012) are as follows:

(1) Construction of the initial sample space matrix and grade standard matrix.

The initial sample space matrix X contains m rows and n columns (Equation 7), where m are the number of groundwater samples, n means the number of evaluation indices, and x_{ij} represents the measurement value of the j th index for the i th water sample.

$$X = \begin{bmatrix} x_{11} & x_{12} & \dots & x_{1n} \\ x_{21} & x_{22} & \dots & x_{2n} \\ \vdots & \vdots & & \vdots \\ x_{m1} & x_{m2} & \dots & x_{mn} \end{bmatrix} \quad (7)$$

Assume F is an attribute space on X , and $(C_1, C_2, C_3, \dots, C_K)$ is an ordered partitioned set of F with the condition $C_1 > C_2 > C_3 > \dots > C_K$. Once the grading criteria of evaluation indices are determined, the grading standard matrix can be expressed as Equation 8:

$$\begin{matrix} & C_1 & C_2 & \dots & C_K \\ \begin{matrix} G_1 \\ G_2 \\ \vdots \\ G_n \end{matrix} & \begin{bmatrix} a_{11} & a_{12} & \dots & a_{1K} \\ a_{21} & a_{22} & \dots & a_{2K} \\ \vdots & \vdots & & \vdots \\ a_{n1} & a_{n2} & \dots & a_{nK} \end{bmatrix} \end{matrix} \quad (8)$$

where a_{jk} ($j=1, 2, \dots, n; k=1, 2, \dots, K$) is the k th partition value of j th index in F , and $a_{j1} < a_{j2} < \dots < a_{jK}$, or $a_{j1} > a_{j2} > \dots > a_{jK}$. Five evaluation indices including Cl^- , TDS, Revelle Index (RI), SO_4^{2-} and Sodium Adsorption ratio (SAR) were selected in this study.

With reference to the Chinese Technical Specification for Seawater Monitoring and Evaluation (HY/T 0314-2021), the Standard for Groundwater Quality (GB/T 14848-2017) and related literature (Zhang et al., 2022), the range and representative value of each evaluation index for different grades were determined and given in Table 1. Based on these evaluation indices and their representative values, the grading standard matrix can be written as Equation 9:

$$\begin{matrix} & I & II & III \\ \begin{matrix} Cl^- \\ TDS \\ RI \\ SO_4^{2-} \\ SAR \end{matrix} & \begin{bmatrix} 100 & 500 & 1500 \\ 500 & 1500 & 4500 \\ 0.5 & 1.5 & 5.7 \\ 50 & 150 & 450 \\ 1.0 & 3.0 & 10.0 \end{bmatrix} \end{matrix} \quad (9)$$

(2) Determination of weight based on Shannon entropy theory.

The initial matrix is normalized to eliminate the incomparability of each index due to different dimensions. The normalization method is as follows:

$$y_{ij} = \frac{(x_{ij})_{max} - x_{ij}}{(x_{ij})_{max} - (x_{ij})_{min}} \quad (10)$$

where $(x_{ij})_{max}$ and $(x_{ij})_{min}$ are the maximum value and the minimum value of j th evaluation indicator in the initial matrix, respectively.

The entropy value of the j th evaluation indicator is:

$$e_j = -\frac{1}{\ln m} \sum_{i=1}^m f_{ij} \ln f_{ij} \quad j = 1, 2, \dots, n \quad (11)$$

$$\text{with } f_{ij} = \frac{y_{ij}}{\sum_{i=1}^m y_{ij}} \quad (12)$$

The weight of index j is calculated as:

$$\omega_j = \frac{1 - e_j}{n - \sum_{j=1}^n e_j} \quad (13)$$

(3) Calculation of attribute measure and attribute recognition.

Suppose $a_{j1} < a_{j2} < \dots < a_{jK}$, the attribute measure of x_{ij} with the attribute C_k is defined as $\mu_{ijk} = \mu(x_{ij} \in C_k)$, and it satisfies Equation 14:

$$\left\{ \begin{array}{l} \mu_{ij1} = 1, \mu_{ij2} = \mu_{ij3} = \dots = \mu_{ijK} = 0, \text{ if } x_{ij} \leq a_{j1} \\ \mu_{ijK} = 1, \mu_{ij1} = \mu_{ij2} = \dots = \mu_{ij(K-1)} = 0, \text{ if } x_{ij} \geq a_{jK} \\ \mu_{ijl} = \frac{|x_{ij} - a_{j(l+1)}|}{|a_{jl} - a_{j(l+1)}|}, \\ \mu_{ij(l+1)} = \frac{|x_{ij} - a_{jl}|}{|a_{jl} - a_{j(l+1)}|}, \text{ if } a_{jl} \leq x_{ij} \leq a_{j(l+1)}, 1 \leq l \leq K - 1 \\ \mu_{ijk} = 0, k < l \text{ or } k > l + 1. \end{array} \right. \quad (14)$$

TABLE 1 Grading criteria and representative values for evaluation indices of groundwater salinization.

Evaluation indices	No salinization Grade I		Minor salinization Grade II		Serious salinization Grade III	
	Range	Representative value	Range	Representative value	Range	Representative value
Cl ⁻ (mg/L)	<250	100	250~1000	500	>1000	1500
TDS(mg/L)	<1000	500	1000~3000	1500	>3000	4500
RI*	<1.0	0.5	1.0~3.6	1.5	>3.6	5.7
SO ₄ ²⁻ (mg/L)	<100	50	100~300	150	>300	450
SAR*	<2.0	1.0	2.0~6.7	3.0	>6.7	10.0

*: note that $RI = \frac{(Cl^-)}{(HCO_3^- + CO_3^{2-})}$, and $SAR = \frac{(Na^+)}{\sqrt{(Ca^{2+} + Mg^{2+})/2}}$ (in meq/l).

Then the attribute measure of i th water sample $\mu_{ik} = \mu(x_i \in C_k)$ considering the weight index is calculated as:

$$\mu_{ik} = \mu(x_i \in C_k) = \sum_{j=1}^n \omega_j \mu_{ijk}, \quad 1 \leq i \leq m, \quad 1 \leq k \leq K \quad (15)$$

According to the confidence criterion, the groundwater salinization grade k_i can be determined by:

$$k_i = \min \left\{ k : \sum_{l=1}^k \mu_{il} \geq \lambda, \quad 1 \leq k \leq K \right\} \quad (16)$$

Generally, the value of λ ranges from 0.6 to 0.75 and it equals 0.65 in this study.

Based on the scoring criteria of attribute recognition, the eigenvalue of groundwater salinization grade (q_{x_i}) is calculated. The larger the eigenvalue, the lower the groundwater salinization grade.

$$q_{x_i} = \sum_{l=1}^K n_l \mu_{il} \quad (17)$$

where $n_l = K + 1 - l$. Finally, x_i can be sorted by the q_{x_i} .

3 Results

3.1 Water type

The hydrochemical facies and water types for water samples have been assessed using Piper diagram as shown in Figure 3. For river water samples, the water type of R5, collected in the upper reaches of the Dalangdian Canal, is $\text{HCO}_3\text{-Ca}$. The river water sample R4 is of Cl-Ca-Mg type. The other three river samples collected in the lower reaches are characterized by the Cl-Na type, indicating that they have been affected by seawater.

For groundwater samples, in summer, three groundwater samples (G2, G3, G6) fall in zone 6, i.e., the $\text{HCO}_3\text{-Ca-Na}$ type. The other groundwater samples fall in zones 2 and 5, and the proportions are 72.7% and 18.2%, respectively. In winter, the sample of D59 fall in zone 1, i.e., the Cl-Ca type. The other groundwater samples also fall in zones 2 and 5, and the

proportions are 68.2% and 27.3%, respectively. These indicate that the groundwater in this area is mainly of Cl-Na type followed by Cl-Ca-Mg type.

3.2 Distributions of GQI_{SWI}

The geostatistical analysis was performed to determine spatial distribution of the GQI_{SWI} in the study area using the ArcGIS Geostatistical Analyst (Nas and Berkta, 2010). The ordinary kriging method was used in this study. The normal distribution pattern has been checked by a histogram tool and normal QQPlots and it was determined that it approximates normal distributions. An analysis trend was made, and it was determined that there is a linear trend along the East-West direction. This trend was removed before kriging interpolations. The 11 different semivariogram models were tested (Supplementary Table S2). From the cross-validation statistics, the Gaussian model is chosen as the final model for summer and the J-Bessel model is chosen for winter.

As indicated by Tomasziewicz et al. (2014), the GQI_{SWI} can range between 0 and 100, where 0 is indicative of seawater and 100 represents freshwater. In general, index values are above 75 for freshwater and below 50 for saline groundwater and seawater. Mixed groundwater has a GQI_{SWI} between 50 and 75.

In summer, values of GQI_{SWI} range from 20.47 to 75.38 with an average of 59.31. Figure 4 shows that values of GQI_{SWI} in the central and western regions are generally above 50, and values of GQI_{SWI} in the eastern coastal area are mostly below 50. Equations 1–5 indicate that the higher the GQI_{SWI} index, the lighter the groundwater salinization degree. In this area, the GQI_{SWI} gradually increases from east to west, indicating that the degree of groundwater salinization is gradually alleviated from coast to inland. The GQI_{SWI} index of the G32 sample, southeast of the study area, achieves the lowest value, highlighting a serious groundwater salinization status there. In winter, values of GQI_{SWI} range from 54.47 to 79.09 with an average of 66.00, slightly higher than that in summer.

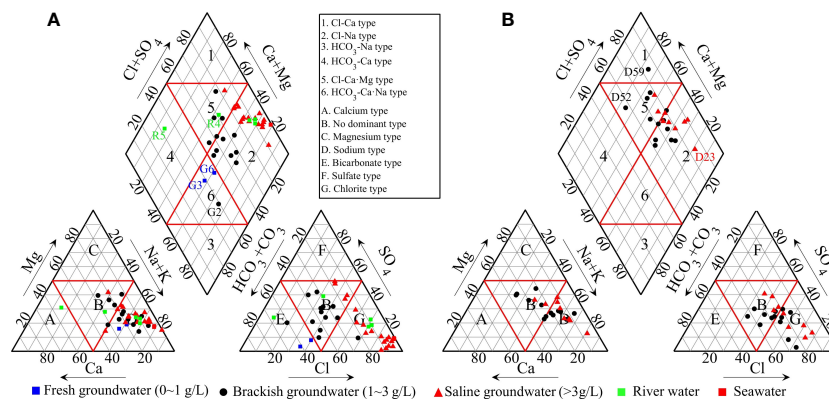


FIGURE 3 Piper diagrams of the collected water samples in summer (A) and winter (B) in Cangzhou, China.

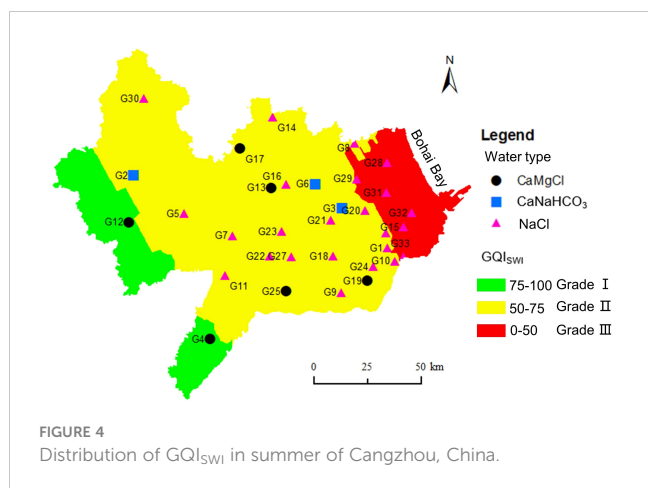


FIGURE 4 Distribution of GQI_{swi} in summer of Cangzhou, China.

3.3 Results of ARMEW

Table 2 gives the calculated weight of evaluation indices according to the measured data and Equations 10–13. Put these weights into Equation 15, the attribute measure of each water sample can be derived (Table 3). The salinization grade is determined by Equation 16, and the corresponding eigenvalue q_x is calculated by Equation 17. Note that the larger the q_x , the lower the groundwater salinization grade. The results indicate that the proportion of no salinization (Grade I), minor salinization (Grade II) and serious salinization (Grade III) identified by ARMEW in groundwater samples in summer in Cangzhou is 3.0%, 21.2% and 75.8%, respectively. In winter, the proportion is 9.1% for Grade II and 90.9% for Grade III.

4 Discussion

4.1 Groundwater evolution mechanisms

There are three main mechanisms controlling the groundwater composition, including atmospheric precipitation, rock dominance, and evaporation-crystallization process (Gibbs, 1970). As shown in Figure 5, all saline groundwater and seawater fall into the zone of evaporation dominance, suggesting the evaporation-crystallization process is of vital importance during saline groundwater evolution. Brackish groundwater are located at the intersection of the evaporation dominance zone and the rock dominance zone, indicating these groundwater samples have been influenced by both effects. The hydrochemistry of the freshwater samples (G3, G6, R4, R5) is dominated by the water-rock interaction. Figure 5A shows that the $Na^+/(Na^+ + Ca^{2+})$ values of groundwater change from 0.406 to 0.997 with an average of 0.759, implying strong cation

TABLE 2 Weights of evaluation indices.

Evaluation indices	Cl ⁻ (mg/L)	TDS (mg/L)	SAR	R	SO ₄ ²⁻ (mg/L)
weight	0.148	0.147	0.230	0.153	0.323

exchange and high background concentration of Na⁺. Figure 5B shows that the $Cl^-/(Cl^- + HCO_3^-)$ values of groundwater range from 0.238 to 0.967 with an average of 0.681. The sample of G2 has the minimum value of $Cl^-/(Cl^- + HCO_3^-)$ and the sample of G32 has the largest value. The evolution from G2 to G32 corresponds to the evolutionary path from the HCO₃ end-member to the Cl end-member, which is in line with the results from Figures 3 and 4.

Figures 6A and C show that Na⁺+K⁺ and Mg²⁺ are mostly distributed along the local seawater dilution line (LSDL), which reflects the mixing between seawater and continental water contributions. The concurrence of the sodium and chloride values with the mixing line is due to the high solubility product of halite, which is considered as the main source of both elements. Figures 6B and D show that most groundwater samples exhibit larger calcium and sulfate content than the expected from the LSDL, and 89% of the samples present a higher Ca²⁺/SO₄²⁻ ratio than that of local seawater (0.43, meq/L ratio). Such a high Ca²⁺/SO₄²⁻ ratio suggests underground gypsum dissolution. Figure 6E shows that the HCO₃⁻ of all groundwater samples are distributed above the LSDL. When the atmospheric precipitation infiltration through the soil zone, the mineral dissolution reactions occur (Appelo and Postma, 2006). Through these reactions, the cations dissolve from rocks into groundwater, increasing the content of cations, while simultaneously increases HCO₃⁻.

The chlor-alkaline indices (CAI-I and CAI-II; Equation 18, 19) were used to further study the cation exchange process of groundwater (Schoeller, 1984):

$$CAI - I = (Cl^- - (Na^+ + K^+))/Cl^- \tag{18}$$

$$CAI - II = (Cl^- - (Na^+ + K^+))/(HCO_3^- + SO_4^{2-} + CO_3^- + NO_3^-) \tag{19}$$

Figure 6F shows that in summer and in winter, 84.6% and 61.5% of brackish groundwater present negative chlor-alkaline indices. This indicates that Ca²⁺ and Mg²⁺ in these brackish groundwater are being replaced by Na⁺ and K⁺ in aquifers, i.e., direct cation exchange. Positive chlor-alkaline indices account for 72.2% in summer and 44.4% in winter of saline groundwater, indicating the reverse cation exchange occurs during seawater intrusion for these saline samples (Appelo and Postma, 2006; Giménez-Forcada, 2010). For the whole year, negative chlor-alkaline indices have a slight advantage than the positive ones, as the percentage of negative ones accounts for 56.4% of the total groundwater samples.

The HFE-D was plotted to further investigate the cation-exchange process during seawater intrusion and freshening (Figure 7). Here, freshwater belong to Ca-HCO₃ facies (13), and seawater correspond to Na-Cl facies (4). In summer (Figure 7A), about 41.5% of total water samples follow the mixing line, suggesting an ideal mixing between freshwater and seawater without ionic exchange for these samples. Most saline groundwater samples, represented by G20, G29, and G31, exhibit compositions following Trend 1. Particularly, the proportion of Na⁺+K⁺ and Ca²⁺ of the groundwater sample G19 is 33.4% and 27.2%, respectively. It is very close to the Ca-Cl facies, implying the

TABLE 3 Attribute measure and seawater intrusion grades.

No.	Attribute measure			Grade	Eigenvalue q_{x_i}	No.	Attribute measure			Grade	Eigenvalue q_{x_i}
	I	II	III				I	II	III		
G1	0.169	0.154	0.677	III	1.492	G18	0.000	0.066	0.934	III	1.066
G2	0.320	0.377	0.303	II	2.017	G19	0.000	0.738	0.262	II	1.738
G3	0.713	0.273	0.014	I	2.699	G20	0.323	0.000	0.677	III	1.646
G4	0.202	0.628	0.170	II	2.032	G21	0.000	0.000	1.000	III	1.000
G5	0.111	0.555	0.333	II	1.778	G22	0.000	0.317	0.683	III	1.317
G6	0.580	0.335	0.085	II	2.494	G23	0.000	0.092	0.908	III	1.092
G7	0.108	0.272	0.621	III	1.487	G24	0.000	0.000	1.000	III	1.000
G8	0.124	0.428	0.448	III	1.676	G25	0.000	0.387	0.613	III	1.387
G9	0.171	0.726	0.103	II	2.067	G26	0.000	0.098	0.902	III	1.098
G10	0.164	0.745	0.091	II	2.073	G27	0.000	0.103	0.897	III	1.103
G11	0.106	0.409	0.485	III	1.622	G28	0.000	0.000	1.000	III	1.000
G12	0.109	0.485	0.406	III	1.703	G29	0.000	0.000	1.000	III	1.000
G13	0.000	0.531	0.469	III	1.531	G30	0.000	0.427	0.573	III	1.427
G14	0.000	0.369	0.631	III	1.369	G31	0.000	0.000	1.000	III	1.000
G15	0.000	0.125	0.875	III	1.125	G32	0.000	0.000	1.000	III	1.000
G16	0.000	0.193	0.807	III	1.193	G33	0.000	0.000	1.000	III	1.000
G17	0.252	0.330	0.417	III	1.835						
D13	0.000	0.000	1.000	III	1.000	D57	0.000	0.298	0.702	III	1.298
D21	0.000	0.508	0.492	III	1.508	D58	0.000	0.422	0.578	III	1.422
D22	0.000	0.252	0.748	III	1.252	D59	0.020	0.444	0.536	III	1.484
D23	0.000	0.235	0.765	III	1.235	D60	0.150	0.461	0.389	III	1.761
D33	0.312	0.269	0.419	III	1.893	D61	0.000	0.330	0.670	III	1.330
D51	0.016	0.369	0.615	III	1.401	D62	0.000	0.002	0.998	III	1.002
D52	0.395	0.531	0.074	II	2.321	D63	0.108	0.801	0.091	II	2.016
D53	0.038	0.601	0.362	III	1.676	D64	0.000	0.450	0.550	III	1.450
D54	0.000	0.296	0.704	III	1.296	D11	0.000	0.447	0.553	III	1.447
D55	0.000	0.460	0.540	III	1.460	D12	0.000	0.505	0.495	III	1.505
D56	0.059	0.521	0.421	III	1.638	D32	0.000	0.350	0.650	III	1.350

groundwater sampling points starting with “G” denote groundwater samples collected in summer, and “D” means groundwater samples collected in winter.

advance of the saline front, the same as that shown in Figure 4. Besides, about 42.4% of the total groundwater samples exhibit compositions following Trend 2, i.e., the freshening process. The Na-HCO₃ facies is observed at G2, G3 and G6, indicative of the evident direct cation exchange reactions during the freshening phase. This further proves the result from Figure 6F. In winter (Figure 7B), about 18.2% of groundwater samples follow the mixing line. Three water samples D21, D59, and D63, exhibit significant intrusion trend. Particularly, the proportion of Ca²⁺ and Cl⁻ of D59 is 34.8% and 56.9%, respectively. Therefore, it obviously belongs to the Ca-Cl facies, the same as the result from Piper diagram. Besides, about 54.5% of the groundwater samples follow the freshening

trend, but without obvious Na-HCO₃ facies compared to the summer campaign.

The occurrence of groundwater freshening is based on the existing saline groundwater and soil. As indicated by Figure 2, the density difference between upper saline water and deep fresh water drive the saline water moving downward. This process has become more active under the influence of extracting deep groundwater. As a result, the upper shallow groundwater is becoming fresher (Guo et al., 1995). Also, due to the influence of historical transgressions, there are remains of transgressions preserving in this area, including marine evaporate sources or marine strata. This provided Na-rich soil such as sodium-montmorillonite. It has been reported that the

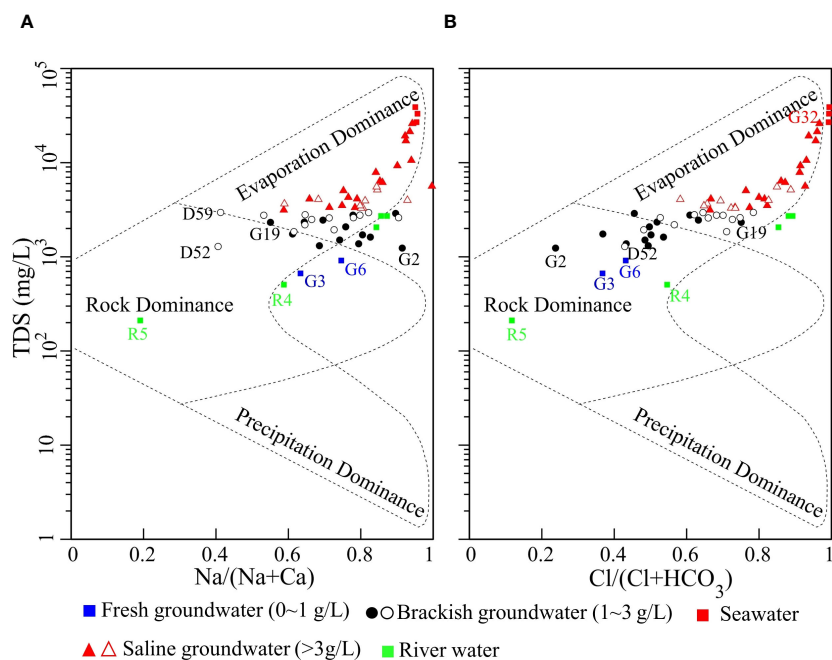


FIGURE 5

Variation of $\text{Na}^+ / (\text{Na}^+ + \text{Ca}^{2+})$ (A) and $\text{Cl}^- / (\text{Cl}^- + \text{HCO}_3^-)$ (B) as a function of TDS. Solid symbols denote water samples collected in summer and hollow symbols denote groundwater samples collected in winter.

main cation of the saline soil in the coastal plain of Cangzhou is Na^+ (He et al., 2021). In recent years, the government has implemented the South-to-North water diversion project and restricted groundwater extractions. Thus, local people generally use delivered surface water for irrigation nowadays. The Ca-HCO_3 river water continuously recharges Ca^{2+} to groundwater. The excess Ca^{2+} and the widespread Na-rich soil together trigger the direct cation exchange.

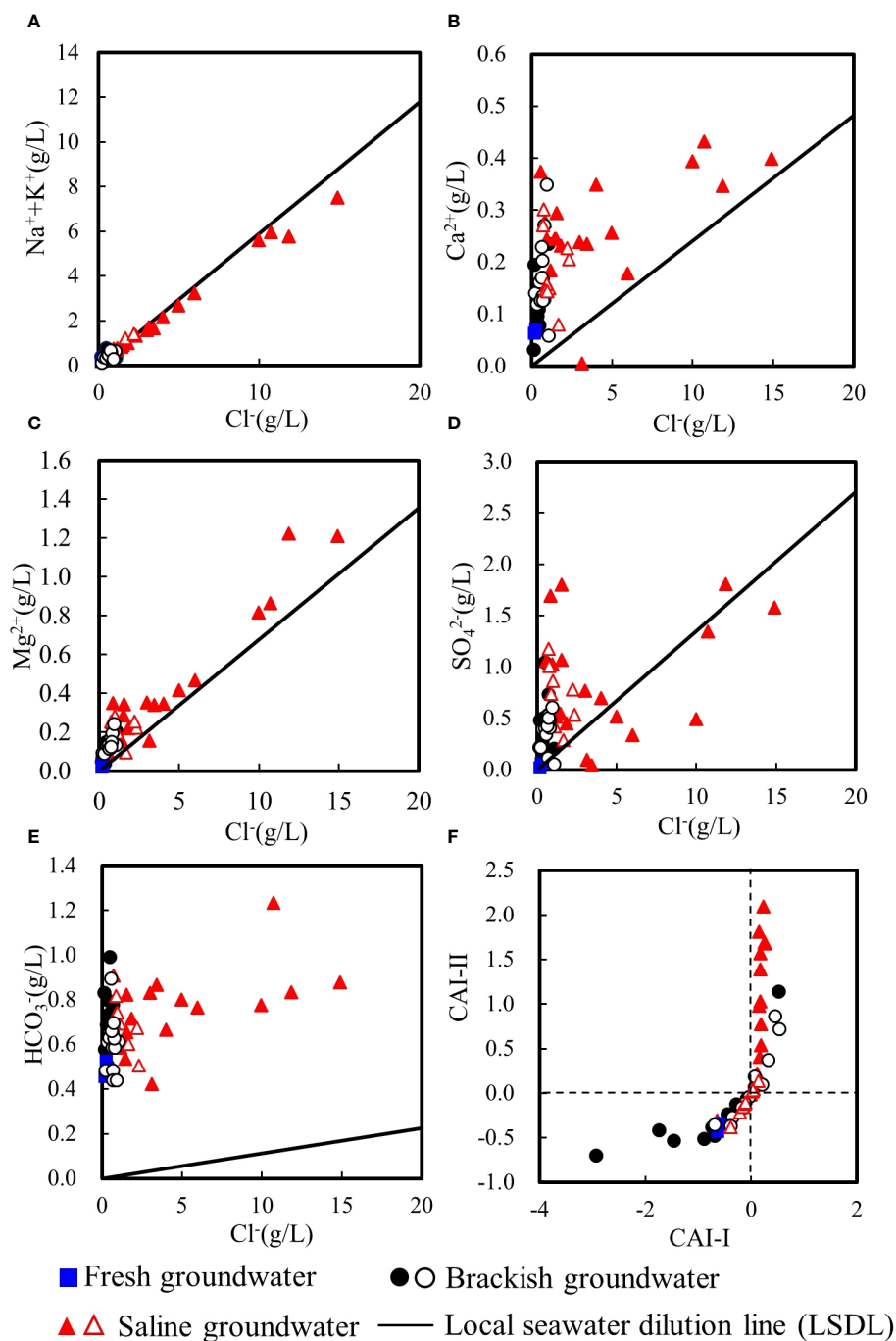
The mineral saturation index (SI) is calculated through PHREEQC to determine the dissolution or precipitation of minerals. It is usually supposed that values in the ± 0.5 range approximate equilibrium status. Figures 8A and B shows that the maximum value for the calculated SI of halite and gypsum is -2.75 and -1.17, respectively, indicating a subsaturation state for the two minerals. This means that groundwater is available to continue dissolving these two minerals from the matrix, and they do not precipitate out of the solution even under the strong effects of evaporation. Figures 8C and D show that the minimum SI value of dolomite and calcite is 1.03 and 0.21, respectively, indicating that they are in an oversaturated state and have a tendency to precipitate, which further aggravates soil hardening. These results agree with the research by Xu et al. (2009).

4.2 Comparison between different methods

Figure 9 shows the percentage of groundwater salinization degree identified by different methods. In summer (Figure 9A), the consistency between the ARMEW and the evaluation method

based on single index of Cl^- is 60.6%, and that between the ARMEW and the GQI_{SWI} index method is 45.5%. The latter two methods gave the same evaluation result for Grade I, and their percentages are less than that estimated by the Cl^- index. The percentage of Grade II determined by the ARMEW is smaller than those determined by the other two methods. The percentage of Grade III determined by the ARMEW is the largest among the three methods. In winter (Figure 9B), for Cl^- and GQI_{SWI} index, the percentage of Grade II has increased by 33.3 and 19.7%, respectively, compared to that in summer. The decrease in the percentage of Grade III identified by these two methods is due to the lack of corresponding sampling points in the eastern part of the study area in the winter campaign. For the result of ARMEW, the percentage of Grade III has increased by 15.1% compared to that in summer. Again, the groundwater salinization degree evaluated by the ARMEW is the highest among the three methods.

Figure 10 shows the spatial distributions of groundwater salinization in Cangzhou based on Cl^- and the ARMEW in summer. It can be seen that the salinization grade generally increases from inland to coast. Combined with Figure 4, the evaluation method based on Cl^- gives the largest area of Grade I. The GQI_{SWI} index shows the largest area of Grade II, and ARMEW presents the largest area of Grade III. In the west of the study area, although Cl^- content is small, TDS or SO_4^{2-} value has reached the level of minor salinization ($\text{TDS} > 1 \text{ g/L}$ or $\text{SO}_4^{2-} > 100 \text{ mg/L}$, Table 1), and thus it belongs to Grade II in Figure 10B. In the middle of this area, although Cl^- content is smaller than 1 g/L , most samples including G7, G11, G16, G22, G23, and G27 have a SAR value higher than 6.7, which reaches the level of serious salinization.

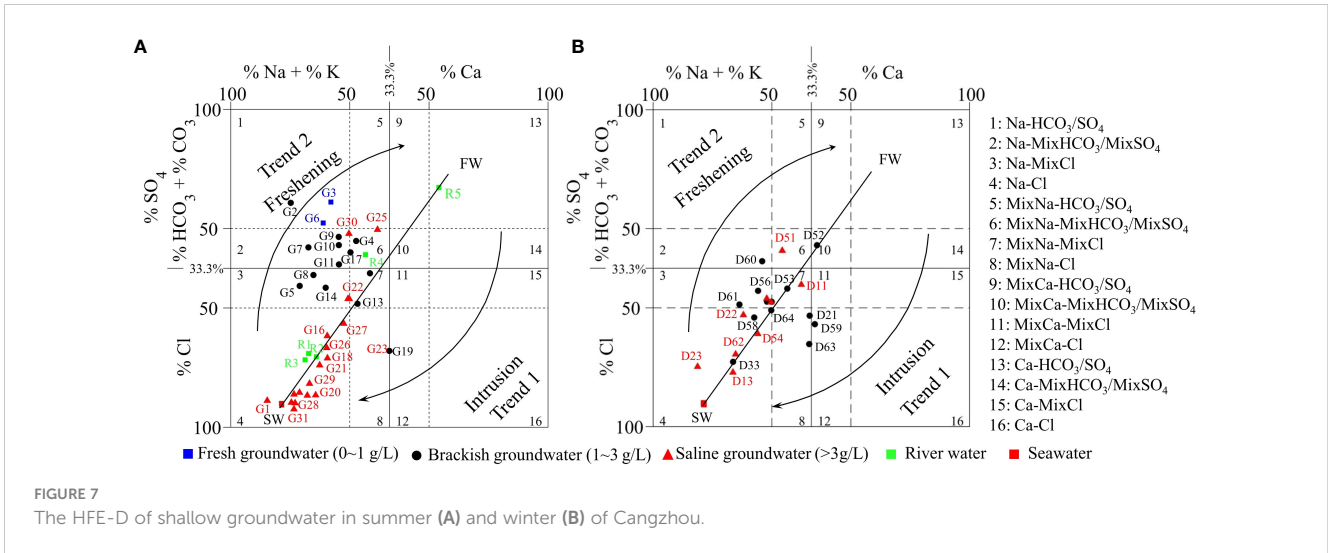


All the three methods demonstrate a serious salinization in the east of this area, at least including G15, G28, G29, G31~33.

The spatial distributions of groundwater salinization identified by different methods in winter are given in [Supplementary Figure S1](#). Similar to the result of [Figure 10](#), the GQI_{SWI} index shows the largest area of Grade II, and ARMEW presents the largest area of Grade III. In winter, instead of higher SAR values in summer, the higher grade identified by ARMEW is mainly due to large values of SO_4^{2-} in 81.8% water samples, which exceeds the threshold of 300 mg/L.

5 Conclusions

This study investigated the hydrogeochemical characterization of shallow groundwater and evaluated the groundwater salinization status in both wet and dry seasons in Cangzhou, China. Through the Piper and Gibbs diagrams, the water type and evolution mechanisms of groundwater were analyzed. The groundwater salinization status was determined by both the GQI_{SWI} index and the ARMEW. The trend of de-salinization or salinization of

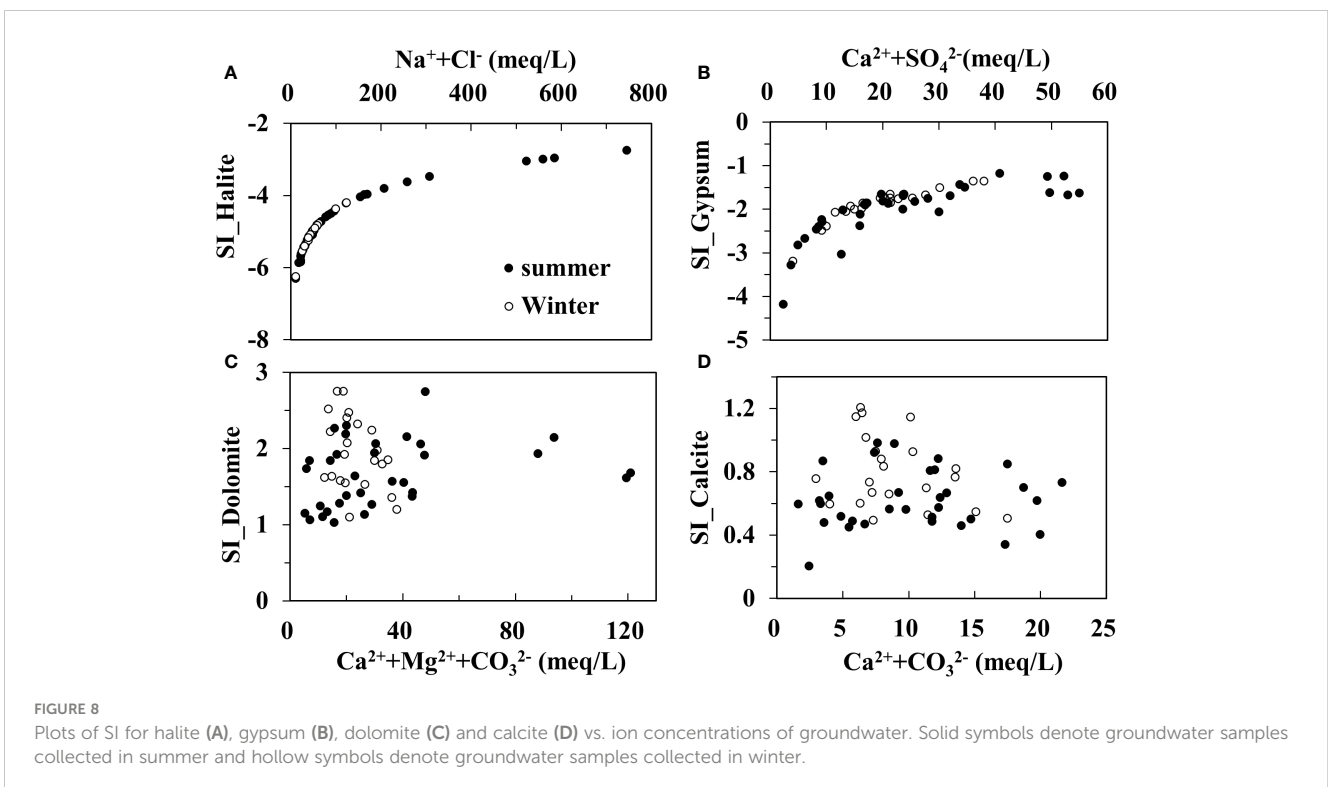


groundwater in this region was determined through the HFE-D. The main conclusions include:

- (1) The hydrochemical types in this area are characterized by Cl-Na and Cl-Ca-Mg. The Gibbs diagram illustrates that the evaporation-crystallization process has significant influence on the evolution of saline groundwater.
- (2) Values of GQI_{SWI} range from 20.47 to 75.38 with an average of 59.31 in summer. The GQI_{SWI} gradually increases from east to west. That is, the degree of groundwater salinization is gradually alleviated from coast to inland. In winter (dry season), values of GQI_{SWI} range

from 54.47 to 79.09 with an average of 66.00, slightly higher than that in summer.

- (3) The proportion of no salinization (Grade I), minor salinization (Grade II) and serious salinization (Grade III) in groundwater samples in summer identified by the ARMEW is 3.0%, 21.2% and 75.8%, respectively. In winter, the proportion is 9.1% for Grade II and 90.9% for Grade III.
- (4) For the whole year, negative chlor-alkaline indices have a slight advantage than the positive ones. The HFE-D diagram reveal that in summer most brackish groundwater exhibit compositions of the freshening stage



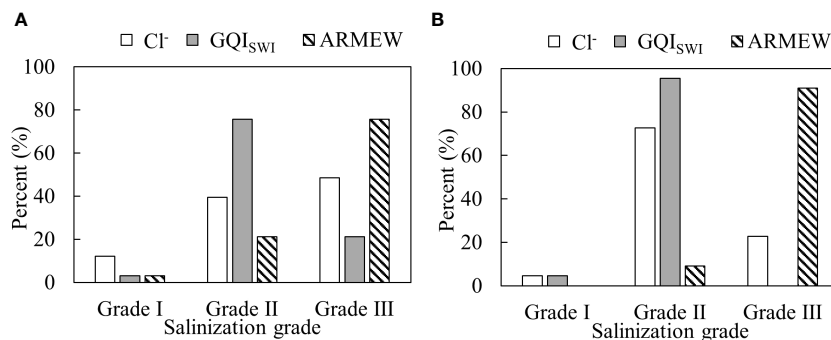


FIGURE 9 Percent of groundwater salinization grades by different methods in summer (A) and in winter (B). For the index of GQI_{SWI}, grades are determined as indicated by Tomaszkiwicz et al. (2014). That is, Grade I: 75~100; Grade II: 50~75; Grade III: 0~50.

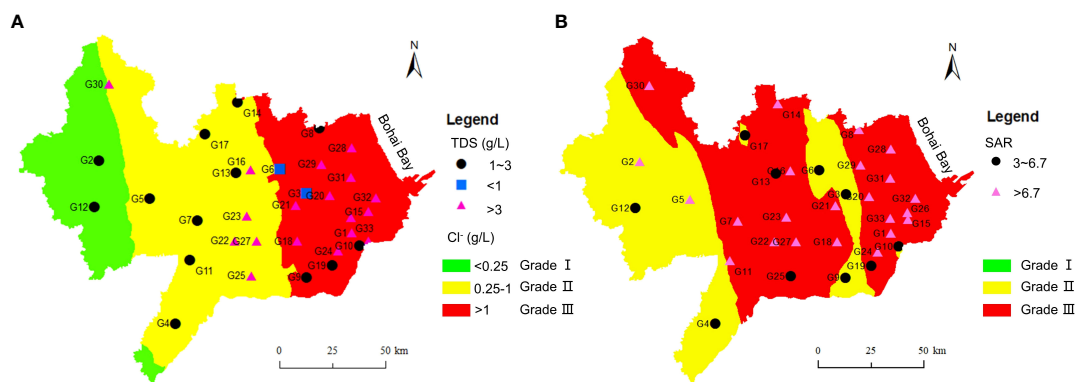


FIGURE 10 Spatial distributions of groundwater salinization degree in Cangzhou based on Cl⁻ (A) and ARMEW (B) in summer.

with direct cation exchange, and most saline groundwater is mainly at the seawater intrusion stage with reverse cation exchange. In winter, compared to the wet summer season, more groundwater samples in the middle of study area exhibit intrusion trend, and without obvious Na-HCO₃ facies.

- (5) Comparison between different methods stresses that the GQI_{SWI} index shows the largest area of Grade II, and ARMEW presents the largest area of Grade III in both seasons. That is, compared with GQI_{SWI} index, ARMEW model gives more conservative evaluation results of groundwater salinization.

This study only analyze the recent status of groundwater salinity distribution. Driven by different factors, the groundwater salinization degree may fluctuate. Since the 1970s and 1980s, large quantities of deep fresh groundwater has been exploited in this area until more than a decade ago, when the government implemented the policies of limited groundwater mining and South-to-North water diversion project. How these human activities have affected the dynamics of groundwater salinity in recent decades remains to be further explored. In addition, this

study only focuses on shallow groundwater, and future studies can evaluate deep groundwater salinization and its vertical connection with shallow groundwater. In spite of these shortcomings, the research results of this study are helpful for evaluating groundwater salinity degree, for understanding the characteristics and evolution mechanisms of brackish and saline groundwater in this area, and for the subsequent research on salinity dynamics.

Data availability statement

The original contributions presented in the study are included in the article/Supplementary Material. Further inquiries can be directed to the corresponding author.

Author contributions

HL: Formal Analysis, Investigation, Writing – original draft. YL: Validation, Visualization, Writing – review & editing. CW: Formal analysis, Methodology, Writing – original draft, Writing – review & editing. KY: Conceptualization, Supervision, Writing –

review & editing. YZ: Funding acquisition, Methodology, Writing – review & editing. XF: Conceptualization, Investigation, Writing – review & editing. XB: Investigation, Visualization, Writing – review & editing. XL: Resources, Visualization, Writing – review & editing.

Funding

The author(s) declare financial support was received for the research, authorship, and/or publication of this article. This work was funded by Science Research Project of Hebei Education Department (ZD2022119), the Natural Science Foundation of Hebei Province of China (D2022403016), the Open Project Program of Hebei Center for Ecological and Environmental Geology Research (No. JSYF-202104), the National Pre-research Funds of Hebei GEO University in 2023 (KY202314), the Central Leading Local Science and Technology Development Fund Project (236Z4204G), Funding for basic scientific research of universities in Hebei Province (QN202212), Science and technology innovation team project of Hebei GEO University (KJCXTD-2021-14).

References

- Appelo, C. A. J., and Postma, D. (2006). *Geochemistry, Groundwater and Pollution*. 2nd ed (Rotterdam: AA Balkema).
- Banks, E. W., Post, V. E. A., Meredith, K., Ellis, J., Cahill, K., Noorduijn, S., et al. (2021). Fresh groundwater lens dynamics of a small bedrock island in the tropics, Northern Australia. *J. Hydrol.* 595, 125942. doi: 10.1016/j.jhydrol.2020.125942
- Benaafi, M., Abba, S. I., and Aljundi, I. H. (2023). State-of-the-art on the conceptual advancement of seawater intrusion: A comprehensive review, management, and possible future research direction. *J. King Saud. Univ.-Sci.* 35, 102749. doi: 10.1016/j.jksus.2023.102749
- Benaafi, M., Tawabini, B., Abba, S. I., Humphrey, J. D., Al-Areeq, A. M., Alhulaibi, S. A., et al. (2022). Integrated hydrogeological, hydrochemical, and isotopic assessment of seawater intrusion into coastal aquifers in Al-Qatif Area, Eastern Saudi Arabia. *Molecules* 27, 6841. doi: 10.3390/molecules27206841
- Bless, A. E., Colin, F., Crabit, A., Devaux, N., Philippon, O., and Follain, S. (2018). Landscape evolution and agricultural land salinization in coastal area: A conceptual model. *Sci. Total Environ.* 625, 647–656. doi: 10.1016/j.scitotenv.2017.12.083
- Boyacioglu, H. (2007). Development of a water quality index based on a European classification scheme. *Afr. J. Online (AJOL)* 33, 101–106. doi: 10.4314/wsa.v33i1.47882
- Cao, T., Han, D., and Song, X. (2021). Past, present, and future of global seawater intrusion research: A bibliometric analysis. *J. Hydrol.* 603, (PA). doi: 10.1016/j.jhydrol.2021.126844
- ChaChadi, A. G., and Lobo-Ferreira, J. P. (2001). "Sea water intrusion vulnerability mapping of aquifers using GALDIT method," in *Proc. workshop on modelling in hydrogeology* (Anna University, Chennai), 143–156.
- Chen, J., Yan, Y., Wang, M., Wang, H., and Li, W. (2015). Temporal-spatial patterns and evolution mechanism of groundwater salinity in groundwater of Cangzhou Area, Hebei Province, China. *Earth Environ.* 43, 522–528. doi: 10.14050/j.cnki.1672-9250.2015.05.006
- Cheng, Q. (1997). Attribute recognition theoretical model with application. *Acta Scientiarum Naturalium Universitatis Pekinensis* 33, 12–20. doi: 10.13209/j.0479-8023.1997.002
- Dhakate, R., Ratnal, G. V., and Sankaran, S. (2020). Hydrogeochemical and isotopic study for evaluation of seawater intrusion into shallow coastal aquifers of Udipi District, Karnataka, India. *Geochem.* 80, 125647. doi: 10.1016/j.chemer.2020.125647
- Essink, G. (2001). Improving fresh groundwater supply-problems and solutions. *Ocean Coast. Manage.* 44, 429–449. doi: 10.1016/S0964-5691(01)00057-6
- Gang, S., Jia, T., Wang, B., Cheng, X., Deng, Y., Han, Y., et al. (2019). Assessment of seawater intrusion in Laoshan district of Qingdao city by using model of set pair analysis based on entropy weight method. *Mar. Environ. Sci.* 38, 939–944 + 976. doi: 10.13634/j.cnki.mes.2019.06.018
- Ghiglieri, G., Carletti, A., and Pittalis, D. (2012). Analysis of salinization processes in the coastal carbonate aquifer of Porto Torres (NW Sardinia, Italy). *J. Hydrol.* 432–433, 43–51. doi: 10.1016/j.jhydrol.2012.02.016
- Gibbs, R. J. (1970). Mechanisms controlling world water chemistry. *Science* 170, 1088–1090. doi: 10.1126/science.170.3962.1088
- Giménez-Forcada, E. (2010). Dynamic of sea water interface using hydrochemical facies evolution diagram. *Groundwater* 48, 212–216. doi: 10.1111/j.1745-6584.2009.00649.x
- Guo, Y., Shen, Z., and Zhong, Z. (1995). Brackish water migration and its relationship with shallow brackish water desalination in Hebei Plain. *Hydrogeol. Eng. Geol.* 22, 8–12. doi: 10.16030/j.cnki.issn.1000-3665.1995.02.003
- Han, D., Kohfahl, C., Song, X., Xiao, G., and Yang, J. (2011). Geochemical and isotopic evidence for palaeo-seawater intrusion into the south coast aquifer of Laizhou Bay, China. *Appl. Geochem.* 26, 863–883. doi: 10.1016/j.apgeochem.2011.02.007
- He, J., Den, Q., Ma, X., Su, X., and Ma, X. (2021). Soil salinization affected by hydrogeochemical processes of shallow groundwater in Cangzhou City, a coastal region in North China. *Hydrol. Res.* 52, 1116–1131. doi: 10.2166/nh.2021.183
- Icaga, Y. (2007). Fuzzy evaluation of water quality classification. *Ecol. Indic.* 7, 710–718. doi: 10.1016/j.ecolind.2006.08.002
- Jasechko, S., Perrone, D., Seybold, H., Fan, Y., and Kirchner, J. W. (2020). Groundwater level observations in 250,000 coastal US wells reveal scope of potential seawater intrusion. *Nat. Commun.* 11, 3229. doi: 10.1038/s41467-020-17038-2
- Kim, I. H., Chung, I. M., and Chang, S. W. (2021). Development of monthly seawater intrusion vulnerability assessment method using GALDIT. *Water* 13, 1820. doi: 10.3390/w13131820
- Kumar, M., Panday, D. P., Bhagat, C., Herbha, N., and Agarwal, V. (2023). Demystifying the decadal shift in the extent of groundwater in the coastal aquifers of Gujarat, India: A case of reduced extent but increased magnitude of seawater intrusion. *Sci. Total Environ.* 898, 165451. doi: 10.1016/j.scitotenv.2023.165451
- Li, F., Angelini, C., Byers, J. E., Craft, C., and Pennings, S. C. (2022). Responses of a tidal freshwater marsh plant community to chronic and pulsed saline intrusion. *J. Ecol.* 110, 1508–1524. doi: 10.1111/1365-2745.13885
- Li, M., Xia, J., Li, F., and Meng, D. (2012). The application of attribute recognition model based on coefficient of entropy to the assessment of seawater intrusion. *Prog. Geogr.* 31, 324–329. doi: 10.11820/dlkxjz.2012.03.007
- Liu, Q., Li, F., Zhang, Q., Li, J., Zhang, Y., Tu, C., et al. (2014). Impact of water diversion on the hydrogeochemical characterization of surface water and groundwater in the Yellow River Delta. *Appl. Geochem.* 48, 83–92. doi: 10.1016/j.apgeochem.2014.07.009
- Lotfata, A., and Ambinakudige, S. (2020). Degradation of groundwater quality in the coastal aquifers of the USA. *Sustain. Water Res. Manage.* 6, 41. doi: 10.1007/s40899-020-00403-w
- Martínez-Pérez, L., Luquot, L., Carrera, J., Marazuela, M. A., Goyette, T., Pool, M., et al. (2022). A multidisciplinary approach to characterizing coastal alluvial aquifers to improve understanding of seawater intrusion and submarine groundwater discharge. *J. Hydrol.* 607, 127510. doi: 10.1016/j.jhydrol.2022.127510

Conflict of interest

The authors declare that the research was conducted in the absence of any commercial or financial relationships that could be construed as a potential conflict of interest.

Publisher's note

All claims expressed in this article are solely those of the authors and do not necessarily represent those of their affiliated organizations, or those of the publisher, the editors and the reviewers. Any product that may be evaluated in this article, or claim that may be made by its manufacturer, is not guaranteed or endorsed by the publisher.

Supplementary material

The Supplementary Material for this article can be found online at: <https://www.frontiersin.org/articles/10.3389/fmars.2024.1384289/full#supplementary-material>

- Moulds, M., Gould, I., Wright, I., Webster, D., and Magnone, D. (2023). Use of electrical resistivity tomography to reveal the shallow freshwater–saline interface in The Fens coastal groundwater, eastern England (UK). *Hydrogeol. J.* 31, 335–349. doi: 10.1007/s10040-022-02586-2
- Moussaoui, I., Rosa, E., Cloutier, V., Neculita, C. M., and Dassi, L. (2023). Chemical and isotopic evaluation of groundwater salinization processes in the Djebeniana coastal aquifer, Tunisia. *Appl. Geochem.* 149, 105555. doi: 10.1016/j.apgeochem.2022.105555
- Nas, B., and Berktaç, A. (2010). Groundwater quality mapping in urban groundwater using GIS. *Environ. Monit. Assess.* 160, 215–227. doi: 10.1007/s10661-008-0689-4
- Saaty, T. L. (1980). *The analytic hierarchy process* (New York: McGraw-Hill).
- Schoeller, H. (1984). *Geochemistry of groundwater. Groundwater studies-an international guide for research and practice* (Paris: UNESCO) 1984, 1–46.
- Stamatis, G., and Voudouris, K. (2003). Marine and human activity influences on the groundwater quality of southern Korinthos area (Greece). *Hydrol. Process.* 17, 2327–2345. doi: 10.1002/hyp.1245
- Tomaszkiewicz, M., NAJM, M. A., and EL-FADEL, M. (2014). Development of a groundwater quality index for seawater intrusion in coastal aquifers. *Environ. Model. Softw.* 57, 13–26. doi: 10.1016/j.envsoft.2014.03.010
- Wang, Z., Wang, S., Liu, W., Su, Q., Tong, H., Xu, X., et al. (2020). Hydrochemical characteristics and irrigation suitability evaluation of groundwater with different degrees of seawater intrusion. *Water* 12, 3460. doi: 10.3390/w12123460
- Wang, X., Zheng, W., Tian, W., Gao, Y., Wang, X., Tian, Y., et al. (2022). Groundwater hydrogeochemical characterization and quality assessment based on integrated weight matter-element extension analysis in Ningxia, upper Yellow River, northwest China. *Ecol. Indic.* 135, 108525. doi: 10.1016/j.ecolind.2021.108525
- Xiong, G., Chen, G., Wu, J., Wang, Z., Yu, H., Fu, T., et al. (2022). Identifying the characteristics and potential risk of seawater intrusion for southern China by the SBM-DEA model. *Sci. Total Environ.* 844, 157205. doi: 10.1016/j.scitotenv.2022.157205
- Xu, Y. (2009). *Geochemistry and ²H and ¹⁸O stable isotopes of Cangzhou aquifer systems.* (PhD thesis). Beijing: China University of Geosciences (Beijing).
- Xu, Y., Tian, X., Zheng, Y., and Li, W. (2009). Increase and decrease in salinity of the shallow groundwater in Cangzhou. *Hydrogeol. Eng. Geol.* 2, 112–116. doi: 10.1287/mksc.1080.0385
- Xue, Y., Wu, J., Liu, P., Wang, J., Jiang, Q., and Shi, H. (1993). Sea-water intrusion in the coastal area of Laizhou Bay, China; 1. Distribution of sea-water intrusion and its hydrochemical characteristics. *Groundwater* 31, 532–537. doi: 10.1111/j.1745-6584.1993.tb00584.x
- Yan, B., Li, X., Hou, J., Bi, P., and Sun, F. (2021). Study on the dynamic characteristics of shallow groundwater level under the influence of climate change and human activities in Cangzhou, China. *Water Supply.* 21, 797–814. doi: 10.2166/ws.2020.308
- Zhang, B., Song, X., Han, D., Guo, Z., Xiao, G., and Yang, J. (2013). Seawater intrusion degree evaluation based on mathematical statistics and fuzzy mathematics in Qinhuangdao Yangdai River Plain. *Scientia Geographica Sin.* 33, 342–348. doi: 10.13249/j.cnki.sgs.2013.03.342
- Zhang, X., Feng, W., and Li, N. (2010). Attribute recognition model based on entropy weight and its application to evaluation of groundwater quality. *Appl. Mech. Mater.* 29–32, 2698–2702. doi: 10.4028/www.scientific.net/AMM.29-32.2698
- Zhang, Y., Li, H., Lian, C., Ding, K., Zhang, W., Shi, L., et al. (2022). Evaluation of seawater intrusion degree in Xingcheng city, Liaoning province by entropy weight method and attribute recognition model. *Mar. Environ. Sci.* 41, 774–782. doi: 10.13634/j.cnki.mes.2022.05.014
- Zhao, J. (1998). Hydrochemical indexes of seawater intrusion and comprehensive judgement on intrusive degree. *Chin. Geographical Sci.* 18, 16–24. doi: 10.1017/S0266078400010713
- Zou, Z., Yun, Y., and Sun, J. (2006). Entropy method for determination of weight of evaluating indicators in fuzzy synthetic evaluation for water quality assessment. *J. Environ. Sci.* 18, 1020–1024. doi: 10.1016/S1001-0742(06)60032-6